

---

# Technetium-99m Hexakis 2-Methoxyisobutyl Isonitrile: Human Biodistribution, Dosimetry, Safety, and Preliminary Comparison to Thallium-201 for Myocardial Perfusion Imaging

Frans J. Th. Wackers, Daniel S. Berman, Jamshid Maddahi, Denny D. Watson, George A. Beller, H. William Strauss, Charles A. Boucher, Michel Picard, B. Leonard Holman, R. Fridrich, Eugenio Inglese, Bernard Delaloye, Angelika Bischof-Delaloye, Leopoldo Camin, and Kenneth McKusick

*The Participating Clinical Centers in the  $^{99m}\text{Tc}$ HEXAMIBI Phase I and II Studies*

The biodistribution, dosimetry, and safety of a new myocardial imaging agent,  $^{99m}\text{Tc}$ -hexakis-2-methoxyisobutyl isonitrile (HEXAMIBI), was evaluated in 17 normal volunteers at rest and exercise (Phase I studies). Technetium-99m HEXAMIBI clears rapidly from the blood with good myocardial uptake and favorable myocardial-to-background ratios for myocardial imaging. Dosimetry allows for administration of up to 30 mCi (1,110 Bq) of [ $^{99m}\text{Tc}$ ]HEXAMIBI. The myocardial images were of good quality and appeared less granular with sharper myocardial walls compared to  $^{201}\text{Tl}$  images. The clinical efficacy of [ $^{99m}\text{Tc}$ ]HEXAMIBI planar stress and rest imaging was evaluated in a multicenter Phase II clinical trial involving 38 patients. Of 36 patients with significant coronary artery disease, 35 patients (97%) had abnormal  $^{201}\text{Tl}$  stress images, and 32 (89%) had abnormal [ $^{99m}\text{Tc}$ ]HEXAMIBI stress images ( $P = \text{N.S.}$ ). Technetium-99m HEXAMIBI images correlated in 31/35 patients (86%) who had either scar or ischemia on  $^{201}\text{Tl}$  images. By segmental myocardial analysis, exact concordance was obtained in 463/570 myocardial segments (81%). This multicenter Phase I and II study indicates that planar [ $^{99m}\text{Tc}$ ]HEXAMIBI stress imaging is safe and compares well with  $^{201}\text{Tl}$  stress imaging for detection of coronary artery disease.

J Nucl Med 30:301-311, 1989

---

**T**echnetium-99m hexakis-2-methoxyisobutyl isonitrile ([ $^{99m}\text{Tc}$ ]HEXAMIBI) is a promising new  $^{99m}\text{Tc}$ -labeled radiopharmaceutical for myocardial perfusion imaging (1-3). Initial experimental studies have shown that [ $^{99m}\text{Tc}$ ]HEXAMIBI is accumulated in the myocardium proportional to the distribution of regional myocardial blood flow, in a manner similar to thallium-201 ( $^{201}\text{Tl}$ ) (4,5). However, unlike  $^{201}\text{Tl}$ , no significant redistribution of the radiopharmaceutical within the myocardium occurs: the initial uptake pattern remains relatively fixed over an extended period of time (6-8).

The present communication describes the results of a multicenter Phase I study on biodistribution, dosimetry, and safety of [ $^{99m}\text{Tc}$ ]HEXAMIBI after injection at rest or during exercise. In addition, results of a multicenter Phase II clinical study on rest-exercise [ $^{99m}\text{Tc}$ ]HEXAMIBI myocardial imaging in comparison to rest-exercise  $^{201}\text{Tl}$  myocardial imaging and coronary angiography are presented.

## METHODS

### Biodistribution and Safety (Phase I Studies)

A total of 17 normal volunteers (16 males, one female) were studied at Yale University, Massachusetts General Hospital, Cedars-Sinai Medical Center, and Brigham & Women's Hospital. The ages ranged from 19 to 49 yr. Upper-body

---

Received May 23, 1988; revision accepted Oct. 27, 1988.

For reprints contact: Frans J. Th. Wackers, MD, Dept. of Diagnostic Radiology-TE-2, Yale University School of Medicine, 333 Cedar St. New Haven, CT 06510.

biodistribution was evaluated in seven subjects: two at rest, two at exercise, and three at rest and exercise. Whole-body biodistribution data were obtained in ten subjects: five at rest, five at exercise. All volunteers were in fasting state. Written informed consent was obtained and the protocols were approved by local institutional review boards.

**Exercise protocol.** Exercise was performed on a motor-driven treadmill using a standard Bruce exercise protocol. All Phase I volunteers exercised to the point of severe fatigue, with a peak exercise heart rate of at least 150 bpm.

**Upper-body imaging.** Upper-body imaging was performed using a standard large field-of-view gamma camera. Technetium-99m HEXAMIBI (7–10 mCi) was injected either at rest (five subjects) or during exercise (five subjects). After the injection during exercise the volunteer was encouraged to continue to exercise for another 2 min. Anterior images were obtained with the heart, lungs, liver, spleen, and gallbladder in the field of view. Sequential 5-min images were obtained beginning 5 min after [<sup>99m</sup>Tc]HEXAMIBI injection and continuing for 60 min. Furthermore, 5-min images were obtained at 120 min, and 180 min after injection.

For evaluation of [<sup>99m</sup>Tc]HEXAMIBI organ distribution and kinetics, regions of interest (ROIs) were selected on the upper-body anterior images including the *entire* visualized liver, spleen, gallbladder, left and right lungs, and left ventricle. The average counts per pixel in each ROI were corrected for decay, and normalized to the initial myocardial count density at 5 min after injection. Organ activity was plotted versus time after injection.

For assessment of *organ ratios*, limited regions of interest (ROIs) (~4–5 pixels in width) were selected over liver, spleen, and right and left lungs *immediately adjacent* to the heart. The average count density over the entire left ventricle was compared to average count density in each of the limited ROI, i.e., heart-to-liver, heart-to-spleen, heart-to-lung ratios. Identical ratios were determined in five <sup>201</sup>Tl studies from our normal database (9).

Thallium-201 exercise imaging usually is performed immediately after exercise and delayed imaging 2–3 hr later, whereas [<sup>99m</sup>Tc]HEXAMIBI imaging in the Phase II study was performed 1 hr after injection either during exercise or at rest. Accordingly, the ratios on [<sup>99m</sup>Tc]HEXAMIBI images, 1 hr after injection during exercise, were compared to the ratios on <sup>201</sup>Tl images, immediately postexercise. Furthermore, the ratios on [<sup>99m</sup>Tc]HEXAMIBI images, 1 hr after injection at rest, were compared to 2–3-hr delayed <sup>201</sup>Tl images.

#### Whole-Body Imaging and Radiation Dosimetry

Whole-body imaging was performed using a standard large field-of-view scanning gamma camera. Anterior and posterior whole-body images were obtained at 5 min, 30 min, 1 hr, 2 hr, 4 hr, and 24 hr after injection of 7–10 mCi of [<sup>99m</sup>Tc]HEXAMIBI either at rest (five subjects) or during exercise (five subjects).

The organ accumulation of [<sup>99m</sup>Tc]HEXAMIBI was determined from the anterior and posterior counts in ROIs over various organs on the whole-body images. The geometric mean organ activity was derived from the square root of the product of anterior and posterior counts. The uptake in each organ was expressed as percent of injected dose, i.e., total organ uptake divided by total-body uptake. In addition, blood samples were drawn at standard time intervals (see below)

during the first 6 hr, and at 24 hr after injection. Furthermore, urine and feces were collected for 24 and 48 hr, respectively.

Data from each subject were fitted separately using linear and nonlinear least squares fitting routines, as subjects often differed in number of resolvable components as well as in the magnitude of the individual parameters. Subjects identified as “stress” or “rest” were segregated, and average residency times (10) for each organ and group were determined. Total-body residence times were determined for each subject from retention predicted by total urinary and fecal excretion. The average total-body residence time minus the average organ residence times gave the residence time for the “remainder of the body” for both subject categories. The appropriate correction for use of radioactivity in the remainder of the body was applied (11). Blood clearance data were not used in performing the radiation dose estimates. Organ dosimetry estimates were calculated by the Radiopharmaceutical Internal Dose Information Center at Oak Ridge Associated Universities.

#### Technetium-99m HEXAMIBI Blood Clearance

To determine blood clearance of the radiopharmaceutical, venous samples were drawn from the arm contralateral to the injection site 30 sec after injection and then as close as possible to each minute during the first 5 min, and then at 10 min, 15 min, 30 min, 1 hr, 4 hr, and 24 hr after injection. The blood samples were counted in a scintillation well counter and specific radioactivity was corrected for decay and expressed as a percentage of injected dose/ml. The half-time clearances at rest and after exercise were calculated by fitting an exponential to six mean data points obtained within the first 5 min as well as to the six mean data points obtained later. No attempt was made to determine actual peak blood activity.

#### Rest-Exercise Imaging in Patients with Coronary Artery Disease (Phase II Studies)

A prospective multicenter Phase II study was carried out in the U.S.A. and Europe (see Appendix) involving 38 patients. To satisfy entry criteria, all patients had both <sup>201</sup>Tl and [<sup>99m</sup>Tc]HEXAMIBI rest-exercise imaging, as well as coronary angiography. The interval between the stress test and cardiac catheterization did not exceed 3 mon. There were 32 men (mean age 59 yr) and six women (mean age 66 yr). Thirty-six patients had significant coronary artery disease by qualitative coronary angiography (>70% luminal stenosis). Sixteen patients had single vessel disease, 11 patients had double vessel disease, and nine patients had triple vessel coronary artery disease. The two remaining patients had normal coronary arteries or insignificant coronary stenoses. Eleven patients had prior myocardial infarction.

#### Exercise Protocol

All patients underwent two exercise tests. Thallium-201 stress imaging was performed first. Employing the Bruce exercise protocol, the first exercise test was symptom limited, whereas the second exercise test was performed to the same double product (heart rate × systolic blood pressure) as that achieved on the first exercise test. End-points for the first exercise test were severe fatigue, angina, >2 mm of ST segment depression, hypotension, or arrhythmias. The radiopharmaceuticals were injected when the patient approached the exercise endpoint. After injection the patient was encouraged to continue to exercise for an additional 1–2 min.

## Myocardial Imaging

Myocardial imaging was performed after i.v. injection of 2 mCi (74 MBq) of  $^{201}\text{Tl}$  at peak exercise. Three-view planar myocardial imaging was performed immediately after termination of exercise and delayed images were obtained 2–3 hr later. Technetium-99m HEXAMIBI imaging was performed at a mean interval of 7.4 days after  $^{201}\text{Tl}$  imaging. For imaging with [ $^{99\text{m}}\text{Tc}$ ]HEXAMIBI, 20–25 mCi (740–925 MBq) were injected at peak exercise and three-view myocardial imaging was performed 1 hr after injection. Resting images were performed 12–24 hr later following a second injection of [ $^{99\text{m}}\text{Tc}$ ]HEXAMIBI (20–25 mCi, 740–925 MBq). Imaging at rest was started 60 min after injection.

In all participating centers, the gamma camera used for  $^{201}\text{Tl}$  imaging was also used for imaging with [ $^{99\text{m}}\text{Tc}$ ]HEXAMIBI. Thallium-201 images were obtained for 8–10 min each, whereas [ $^{99\text{m}}\text{Tc}$ ]HEXAMIBI images were obtained for 5–10 min each.

## Analysis

All studies were stored on magnetic tape or floppy disk and mailed to the Core Laboratory at Yale University, where they were transcribed to a central computer. Image interpretation was performed by visual analysis of unprocessed, analog equivalent, hard copies of computed images. Thallium-201 studies were separated from their companion [ $^{99\text{m}}\text{Tc}$ ]HEXAMIBI studies, and all 38 pairs of images were analyzed blindly by two experienced observers (F.W., D.B.). Consensus, when necessary, was reached by a third reader (J.M.).

For analysis, the left ventricle on each view was divided into five segments, totaling 15 segments per three view study. Each segment was graded as either normal, ischemia (i.e., reversible defect), or scar (i.e., fixed defect). Each segment, furthermore, was assigned to be the territory of a specific coronary artery as proposed previously (12–13).

A three-view patient study was considered to be *normal* if all 15 segments were graded as “normal”, to be *ischemic* if at least one segment was graded as “ischemic,” and to show *scar* if all abnormal segments were graded as “scar.” Studies with the combination of scar and ischemia were, for purposes of this analysis, categorized as “ischemic.”

## Clinical Safety

The volunteers and patients in the Phase I and II studies were observed for adverse reactions and had vital signs (temperature, blood pressure, respiration, heart rate) taken before and 15, 30, 60 min, 4 hr, and 24 hr after injection. Samples for blood chemistry (hemoglobin, hematocrit, complete blood count, sodium, potassium, creatinine, urea, calcium, chloride, SGOT) were drawn before injection, at 60 min, 24 hr, and 2 wk after injection. Urine chemistry was performed on samples obtained at 60 min, 24 hr, and 2 wk after injection. Feces were collected for 48 hr.

## Statistical Analysis

Mean data are given  $\pm$  s.d.

The differences between paired data were analyzed using paired t-test. The differences in detection rate were analyzed using the McNemar test. A probability (p) of  $<0.05$  was considered statistically significant.

The patients in this study were included because of their willingness to perform two exercise tests and because they

underwent (or were going to have) coronary angiography. Therefore, the study patients may not be representative for the general patient population with chest pain syndromes. Consequently, the results of this study will not be described in terms of sensitivity and specificity, but as “*detection rate of coronary artery disease*” and “*identification of absence of coronary artery disease*.”

## RESULTS

### Phase I

#### Image Characteristics

Good quality images were obtained in all normal subjects. Compared to exercise/delayed  $^{201}\text{Tl}$  images, myocardial visualization on exercise/rest [ $^{99\text{m}}\text{Tc}$ ]HEXAMIBI images was similar. However, the [ $^{99\text{m}}\text{Tc}$ ]HEXAMIBI images were less granular and had a “crisper” quality, apparently because of less scatter in comparison to  $^{201}\text{Tl}$  images. During the first 60 min after a *resting injection* (Fig. 1A), marked accumulation of [ $^{99\text{m}}\text{Tc}$ ]HEXAMIBI was present in liver and spleen. Nevertheless, the heart was well visualized. After an *exercise injection* (Fig. 1B), substantially less uptake in the liver and spleen was observed with excellent visualization of heart (right and left ventricle).

Substantial excretion in the gallbladder was noted both after exercise and at rest, reaching a maximum at  $\sim 1$  hr after injection.

#### Blood Clearance

Both rest and postexercise blood decay corrected clearance curves approximate a dual exponential curve with an initial fast and a later slow component.

*Rest.* At 0.5 min after injection, blood activity was  $21.7 \pm 17.6$  of injected dose (I.D.). Maximal activity,  $36 \pm 18\%$  of I.D., was noted at 1 min after injection. Blood activity subsequently decreased to  $23 \pm 0.9\%$  of I.D. at 3 min,  $9 \pm 0.6\%$  of I.D. at 5 min, and  $2.5 \pm 0.3\%$  of I.D. at 10 min after injection. After this time, [ $^{99\text{m}}\text{Tc}$ ]HEXAMIBI blood-pool activity continued to decrease slowly:  $1.3 \pm 0.1\%$  of I.D. at 30 min;  $1.1 \pm 0.01\%$  of I.D. at 60 min;  $0.8 \pm 0.02\%$  of I.D. at 2 hr and  $0.5 \pm 0.03\%$  of I.D. at 4 hr post injection. At 24 hr blood activity was  $0.3 \pm 0.04\%$  of I.D. Curve fitting for the *fast early clearance* at rest gives clearance =  $53.954 \exp(-2.18t)$  (where t is time in minutes). The *slow late clearance* at rest gives clearance =  $1.611 \exp(-0.002t)$ . Thus, the effective  $t_{1/2}$  at rest of the fast early component is 2.18 min.

*Exercise.* Maximal [ $^{99\text{m}}\text{Tc}$ ]HEXAMIBI blood activity ( $51 \pm 28\%$  of I.D.) was measured at 0.5 min after injection during exercise. Blood activity decreased over the following minutes, reaching a level of  $11 \pm 4\%$  of I.D. at 4 min,  $6.5 \pm 2.9\%$  of I.D. at 5 min and  $2.6 \pm 1\%$  of I.D. at 10 min after injection. Subsequently, blood-pool activity continued to decrease slowly:  $1.1 \pm 0.1\%$  of I.D. at 30 min,  $0.7 \pm 0.1\%$  of I.D. at 1 hr,  $0.4 \pm 0.2\%$  of I.D. at 4 hr, and  $0.3 \pm 0.3\%$  of I.D. at 24 hr

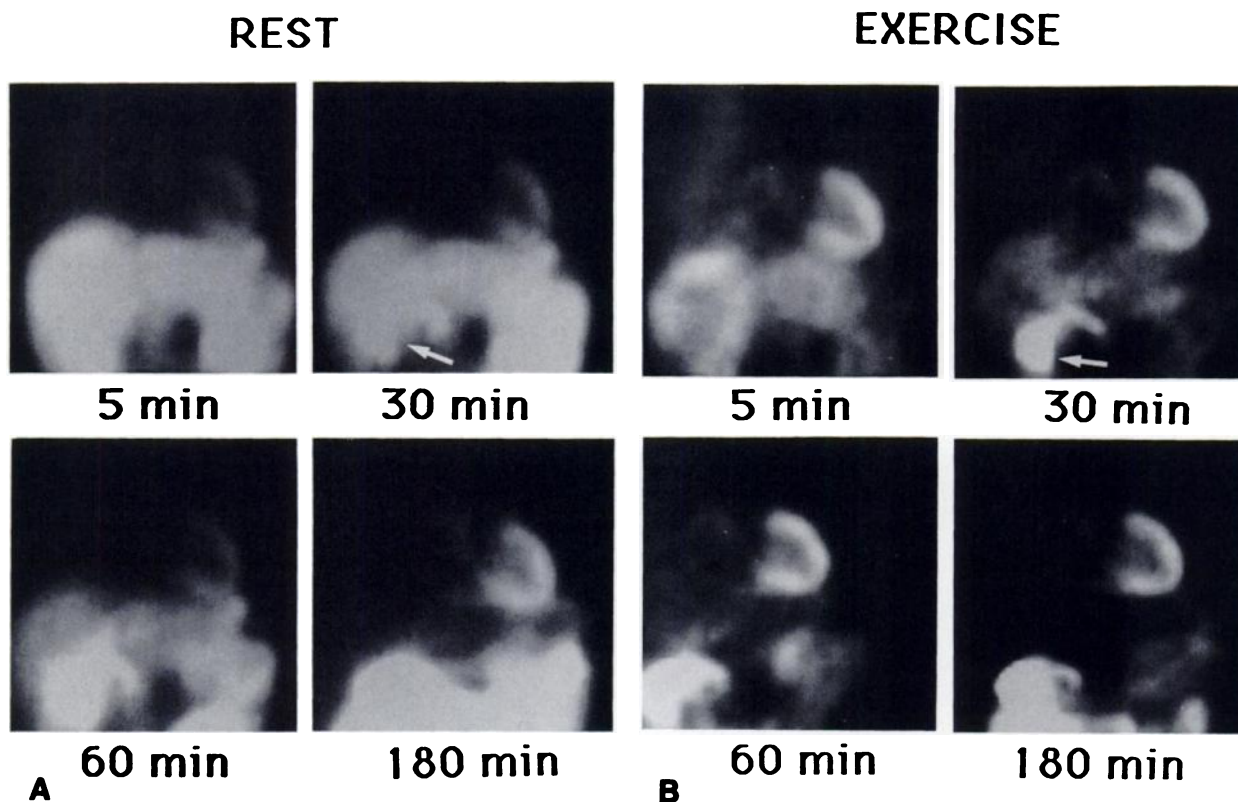


**FIGURE 1**  
**A:** Large field-of-view anterior projections at 5 min, 25 min, 30 min, and 180 min after injection of [<sup>99m</sup>Tc]HEXAMIBI at rest in a normal volunteer. The left ventricle is well visualized. However, the heart-to-liver ratio improves over time by clearance of the radiotracer from the liver into the biliary system (arrow). **B:** Large field-of-view anterior projection after injection of [<sup>99m</sup>Tc]HEXAMIBI at peak exercise in a normal volunteer. The left ventricle is well visualized at all times. Compared to the injection at rest substantially less liver uptake of radiotracer is present.

after injection. Curve fitting for the *fast early clearance* after exercise gives clearance =  $51.137 \exp(-2.13t)$  and for the *late slow clearance* =  $1.342 \exp(-0.002t)$ . Thus, the effective  $t_{1/2}$  of the initial fast component after an injection during exercise was 2.13 min.

#### Upper-Body Organ Distribution

**Rest.** Initially, the highest [<sup>99m</sup>Tc]HEXAMIBI concentration (count density per pixel) was in gallbladder and liver, followed, in decreasing order of activity per pixel, by heart, spleen, and lungs (Fig. 2A). Decay corrected [<sup>99m</sup>Tc]HEXAMIBI activity in spleen and lung decreased gradually over time, whereas [<sup>99m</sup>Tc]HEXAMIBI activity in the heart remained relatively stable. At 3 hr after injection  $27 \pm 4\%$  of initial activity had cleared from the heart, whereas  $67 \pm 12\%$ ,  $76 \pm 4\%$ , and  $49 \pm 4\%$  had, respectively, cleared from spleen, liver, and lungs. Within the first 30–60 min, liver activity decreased with excretion into the biliary system. Maximal accumulation in the gallbladder occurred at ~60 min postinjection. Consequently, since no significant redistribution of [<sup>99m</sup>Tc]HEXAMIBI occurs, with regard to laboratory logistics and patient flow, a convenient and practical time for imaging after injection is ~1 hr after injection. However, with increasing time

interval, the relative visualization of the heart continued to improve. From ~1.5 hr after injection at rest, the count density in the heart was higher than in the immediately adjacent organs. Only the gallbladder had much higher count density.

**Exercise.** Immediately after injection of [<sup>99m</sup>Tc]HEXAMIBI the highest concentration (count density per pixel) was in the gallbladder, followed by heart, liver, spleen, and lungs (Fig. 2B). The cardiac, pulmonary, and splenic activity gradually decreased over time. Hepatic activity decreased more rapidly due to excretion in the biliary system, than any other organ during the first hour. By 3 hr after injection,  $26 \pm 12\%$  of initial cardiac activity had cleared; at this time,  $65 \pm 7\%$  had cleared from the liver,  $43 \pm 21\%$  from the spleen and  $39 \pm 10\%$  from the lungs. At all times after injection during exercise, the count density within the heart was higher than in the immediately adjacent organs. Only the gallbladder had higher count density.

#### Heart-to-Organ Ratios

The ratios of count density between the heart and adjacent organs are relevant for image quality. These ratios determined from limited regions of interest in lung, liver, and spleen immediately adjacent to the heart

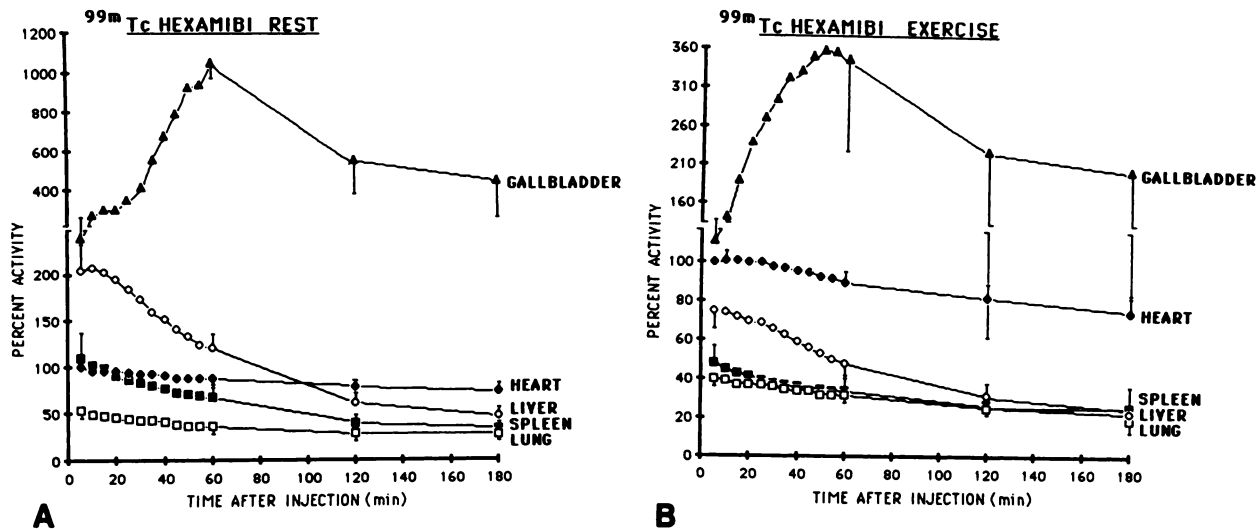


**FIGURE 2**  
 A: Organ time-activity curves after injection at rest in five normal volunteers (mean  $\pm$  s.d.). The data are normalized to cardiac activity at 5 min after injection. For clarity standard deviations are only shown at 5, 60, 120, and 180 min. B: Organ time-activity curves in five normal volunteers after injection during exercise (see text). The format is the same as in Figure 2A.

are shown in Table 1. Comparing the ratios at the actual time of image acquisition, the resting [ $^{99m}\text{Tc}$ ] HEXAMIBI heart-to-liver and heart-to-spleen ratios were significantly less than the corresponding ratios on delayed  $^{201}\text{Tl}$  images ( $p < 0.05$ ). On the other hand, the resting [ $^{99m}\text{Tc}$ ]HEXAMIBI heart-to-lung ratio was greater than that on delayed  $^{201}\text{Tl}$  images ( $p < 0.05$ ). All exercise ratios were not significantly different for the two radiopharmaceuticals.

**Organ Dosimetry**

Organ dosimetry was determined from whole body images by expressing specific organ uptake as percent of injected dose (Table 2). The uptake in the heart was  $1.0 \pm 0.4\%$  of I.D. at 60 min after injection at rest. This was  $1.4 \pm 0.3\%$  of I.D. at 60 min after injection during exercise. The 24-hr urinary excretion was 29.5% of I.D. at rest and 24.1% of I.D. after exercise. The 48-hr fecal excretion was 36.9% of I.D. at rest and 29.1% of I.D.

after exercise. Organ dosimetry is shown in Table 3. The organs involved in the excretory pathways of [ $^{99m}\text{Tc}$ ]HEXAMIBI (gallbladder, intestines, kidneys, and bladder) receive the highest absorbed dose per unit injected radioactivity, with the upper large intestine receiving the highest dose both at rest and after exercise. Some notable dose sparing occurs for the urinary bladder (and gonads, although to a lesser extent) when urinary bladder voiding frequency is increased. It appears that 30 mCi (1,110 MBq) can be administered with no individual organ dose exceeding 5 rad (50 mGy) and most being below 3 rad (30 mGy). The whole-body dose would range from 0.46 rad (rest) to 0.49 rad (exercise).

**Clinical Safety**

Vital parameters, heart rate, blood pressure, electrocardiogram, and blood chemistry were monitored in all volunteers for 24 hr after injection of [ $^{99m}\text{Tc}$ ]HEX-

**TABLE 1**  
 Heart to Organ Ratios for [ $^{99m}\text{Tc}$ ]HEXAMIBI and  $^{201}\text{Tl}$

Time after injection	Heart/liver		Heart/lung		Heart/spleen		No. subjects
	R	EX	R	EX	R	EX	
<b>[<math>^{99m}\text{Tc}</math>]HEXAMIBI</b>							
5 min	$0.5 \pm 0.1$	$1.3 \pm 0.1$	$1.9 \pm 0.2$	$2.1 \pm 0.1$	$0.9 \pm 0.2$	$2.0 \pm 0.4$	5
30 min	$0.5 \pm 0.1$	$1.4 \pm 0.2$	$2.2 \pm 0.1$	$2.3 \pm 0.2$	$1.2 \pm 0.4$	$2.3 \pm 0.3$	5
60 min	$0.6 \pm 0.1$	$1.8 \pm 0.3$	$2.4 \pm 0.1$	$2.4 \pm 0.2$	$1.3 \pm 0.3$	$2.5 \pm 0.3$	5
120 min	$1.1 \pm 0.1$	$2.3 \pm 0.3$	$2.5 \pm 0.1$	$2.5 \pm 0.3$	$1.9 \pm 0.5$	$3.0 \pm 0.7$	5
180 min	$1.4 \pm 0.2$	$2.4 \pm 0.3$	$2.7 \pm 0.2$	$2.5 \pm 0.3$	$1.9 \pm 0.6$	$3.0 \pm 0.9$	5
$^{201}\text{Tl}^*$	$1.4 \pm 0.3^\dagger$	$2.1 \pm 0.3^\ddagger$	$1.9 \pm 0.1^\dagger$	$2.3 \pm 0.2^\ddagger$	$2.3 \pm 0.4^\dagger$	$2.9 \pm 0.6^\ddagger$	5

\* R 2 hr after injection (delayed imaging), EX immediately (20 min) after injection.

†  $p < 0.05$ ; ‡  $p = \text{NS}$  compared to [ $^{99m}\text{Tc}$ ]hexamibi at 60 min after injection.

R = rest, EX = exercise.

**TABLE 2**  
 $[^{99m}\text{Tc}]$ HEXAMIBI Human Biodistribution (% Injected Dose, mean  $\pm$  s.d.)

Time postinjection Organ	5 min		60 min		240 min	
	Rest	Exercise	Rest	Exercise	Rest	Exercise
Heart	1.2 $\pm$ 0.4	1.5 $\pm$ 0.4	1.0 $\pm$ 0.4	1.4 $\pm$ 0.3	0.8 $\pm$ 0.3	1.0 $\pm$ 0.3
Lung	2.6 $\pm$ 0.8	2.7 $\pm$ 2.1	0.9 $\pm$ 0.5	1.4 $\pm$ 1.2	0.4 $\pm$ 0.5	0.3 $\pm$ 0.6
Liver	19.6 $\pm$ 7.1	5.9 $\pm$ 2.9	5.6 $\pm$ 1.6	2.4 $\pm$ 1.6	0.7 $\pm$ 0.5	0.3 $\pm$ 0.3
Gallbladder	1.2 $\pm$ 1.5	0.6 $\pm$ 0.6	3.5 $\pm$ 2.5	2.5 $\pm$ 1.5	2.7 $\pm$ 4.1	2.6 $\pm$ 2.3
Kidney	13.6 $\pm$ 0.9	10.6 $\pm$ 2.2	6.7 $\pm$ 0.7	6.7 $\pm$ 3.9	3.9 $\pm$ 1.2	3.3 $\pm$ 1.0
Thyroid	0.2 $\pm$ 0.07	0.06 $\pm$ 0.06	0.2 $\pm$ 0.06	0.2 $\pm$ 0.2	0.1 $\pm$ 0.04	0.1 $\pm$ 0.1
Legs (Muscle)	10.1 $\pm$ 1.4	21.2 $\pm$ 5.3	11.1 $\pm$ 1.0	22.2 $\pm$ 5.7	10.9 $\pm$ 0.9	22.5 $\pm$ 6.0
Bladder	5.6 $\pm$ 1.8	2.5 $\pm$ 0.9	8.7 $\pm$ 4.2	6.3 $\pm$ 0.7	2.6 $\pm$ 3.0	0.9 $\pm$ 0.8
Spleen	2.5 $\pm$ 0.9	1.0 $\pm$ 0.5	1.0 $\pm$ 0.9	0.4 $\pm$ 0.3	0.1 $\pm$ 0.1	0.1 $\pm$ 0.1

AMIBI. None of the volunteers had either adverse reactions, significant electrocardiographic changes, or blood chemistry changes, which could be attributed to the radiopharmaceutical. Occasionally a transient metallic taste was noted immediately after the injection.

### Phase II

**Exercise.** The double product (heart rate  $\times$  systolic blood pressure) for  $^{201}\text{Tl}$  and  $[^{99m}\text{Tc}]$ HEXAMIBI studies was respectively  $21.84 \times 10^3$  and  $21.48 \times 10^3$  ( $p = \text{N.S.}$ ). Thirty patients (80%) had reproducible symptoms during both tests, i.e., angina (13 patients), ST-segment depression (six patients), angina and ST-segment depression (nine patients), dyspnea (five patients), fatigue (three patients), or arrhythmias (two patients).

**Image characteristics.** In general, the exercise  $[^{99m}\text{Tc}]$ HEXAMIBI images were of excellent quality and visually superior (with respect to less granular appearance

and sharper myocardial walls) (Figs. 3 and 4) in comparison to  $^{201}\text{Tl}$  images. The exercise  $[^{99m}\text{Tc}]$ HEXAMIBI images were comparable to the  $^{201}\text{Tl}$  images with regard to relative distribution of radioactivity and heart-to-lung and heart-to-liver ratios (Table 1). However, the resting  $[^{99m}\text{Tc}]$ HEXAMIBI studies showed significantly higher liver and spleen uptake than the companion  $^{201}\text{Tl}$  redistribution images. Nevertheless, this increased subdiaphragmatic activity did not interfere with image interpretation.

### Comparison to Coronary Angiography

Of 36 patients with significant coronary artery disease, 35 patients had abnormal  $^{201}\text{Tl}$  images and 32 had abnormal  $[^{99m}\text{Tc}]$ HEXAMIBI images (detection rate of 97% and 89% respectively,  $p = \text{N.S.}$ ). The two patients with insignificant coronary artery disease had both normal  $^{201}\text{Tl}$  and  $[^{99m}\text{Tc}]$ HEXAMIBI images.

Of a total of 114 arteries in 38 patients, 65 arteries had significant stenoses, 49 had insignificant lesions or were normal. Of 65 myocardial supply areas with coronary artery disease, 45 (69%) were abnormal by  $^{201}\text{Tl}$  and 39 (60%) by  $[^{99m}\text{Tc}]$ HEXAMIBI stress imaging ( $p = \text{N.S.}$ ). Of 49 myocardial supply areas with normal coronary arteries, 40 (82%) were normal by  $^{201}\text{Tl}$  and 38 (78%) by  $[^{99m}\text{Tc}]$ HEXAMIBI imaging ( $p = \text{N.S.}$ ). There was also no significant difference between detection rate of coronary artery disease or identification of the absence of disease for each of the specific coronary artery supply regions (Figs. 5A and 5B).

### Comparison to $^{201}\text{Tl}$ Imaging

Of a total of 38 patients, 32 (84%) patients had abnormal  $[^{99m}\text{Tc}]$ HEXAMIBI stress-rest images (scar (16%), ischemia (68%)), whereas 35 (92%) patients had abnormal  $^{201}\text{Tl}$  studies (scar (8%), ischemia (84%)), ( $p = \text{N.S.}$  for both scar and ischemia). Of 32 abnormal  $[^{99m}\text{Tc}]$ HEXAMIBI studies, 31 were also abnormal on  $^{201}\text{Tl}$  images. However, of six normal  $[^{99m}\text{Tc}]$ HEXAMIBI studies, four were abnormal on  $^{201}\text{Tl}$  images. Thus, perfect concordance occurred in 29/38 (76%) of patients, whereas concordance regarding normality or abnormality occurred in 33/38 (87%) (Fig. 6).

**TABLE 3**  
Radiation Dose Estimates for  $[^{99m}\text{Tc}]$ HEXAMIBI\*

Organ	Absorbed dose in rad/30 mCi (mGy/1,110 MBq)			
	Stress		Rest	
Gallbladder wall	2.89	(28.9)	2.44	(24.4)
Small intestine	2.78	(27.8)	2.89	(28.9)
Upper large intestine	4.66	(46.6)	4.77	(47.7)
Lower large intestine	3.22	(32.2)	3.33	(33.3)
Heart wall	0.57	(5.7)	0.53	(5.3)
Kidneys	1.67	(16.7)	2.01	(20.0)
Liver	0.43	(4.3)	0.59	(5.9)
Lungs	0.26	(2.6)	0.28	(2.8)
Spleen	0.48	(4.8)	0.60	(6.0)
Thyroid	0.81	(8.0)	0.63	(6.3)
Ovaries	1.22	(12.2)	1.33	(13.3)
Testes	0.29	(2.9)	0.31	(3.4)
Red marrow	0.72	(7.2)	0.77	(7.7)
Urinary bladder wall	1.55	(15.5)	1.89	(18.9)
Total body	0.46	(4.6)	0.49	(4.9)

\* Excretion assumed to be 24.1% in urine (2-hr void), 29.1% in feces for stress patients, 29.5% in urine, 36.9% in feces for rest patients. Activity excreted in feces assumed to enter the GI tract at the small intestine.

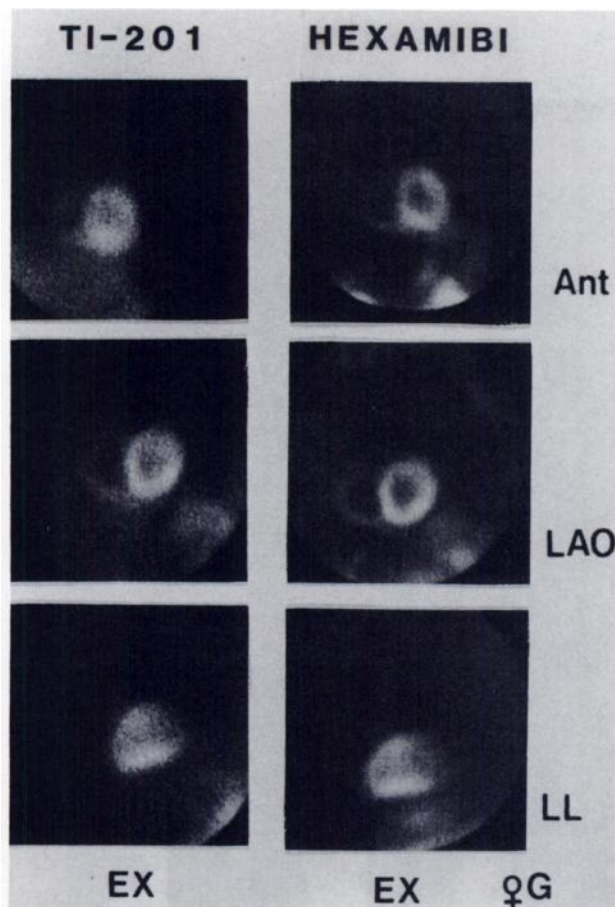


**FIGURE 3**  
Thallium-201 and [<sup>99m</sup>Tc]HEXAMIBI stress images in the same patient (G) in the anterior (ANT), left anterior oblique (LAO), and left lateral (LL) projection. No myocardial perfusion defects are present on either the <sup>201</sup>Tl stress images or the [<sup>99m</sup>Tc]HEXAMIBI stress images. The similarity between the two sets of images, as well as the lesser granular appearance and sharper myocardial walls on the [<sup>99m</sup>Tc]HEXAMIBI images (compared to <sup>201</sup>Tl) can be appreciated.

Using <sup>201</sup>Tl imaging as the standard, [<sup>99m</sup>Tc]HEXAMIBI images identified 86% (31/35) of patients with either scar or ischemia, and 81% (26/32) of patients with ischemia alone.

#### Segmental Analysis

A total of 570 myocardial segments in 38 patients were available for analysis. In 463 (81%) segments, exact segmental concordance was observed between interpretation of <sup>201</sup>Tl and [<sup>99m</sup>Tc]HEXAMIBI images (Fig. 6). Of 453 segments read as normal on [<sup>99m</sup>Tc]HEXAMIBI studies, 64 (14%) were read as abnormal on <sup>201</sup>Tl study, whereas of 410 segments read as normal on <sup>201</sup>Tl studies, 21 (5%) were read as abnormal on [<sup>99m</sup>Tc]HEXAMIBI study. Overall, 43 more segments (8% of all segments) were interpreted as abnormal (either scar or ischemia) on <sup>201</sup>Tl images than on [<sup>99m</sup>Tc]HEXAMIBI images.

## DISCUSSION

The Phase I studies with [<sup>99m</sup>Tc]HEXAMIBI demonstrated favorable biologic properties of [<sup>99m</sup>Tc]HEXAMIBI for myocardial imaging: rapid blood clearance, adequate myocardial uptake, acceptable myocardial-to-background ratios. Compared to <sup>201</sup>Tl (14), [<sup>99m</sup>Tc]HEXAMIBI blood levels immediately after injection are higher, presumably because of lower extraction, whereas late blood levels are lower, presumably because of the lack of redistribution.

Exercise [<sup>99m</sup>Tc]HEXAMIBI images were equal to, and frequently of better quality, i.e., less granular and with sharper myocardial walls, than their companion <sup>201</sup>Tl images. Although resting [<sup>99m</sup>Tc]HEXAMIBI images showed significantly more liver uptake than <sup>201</sup>Tl delayed images, in the present study this did not interfere with the ability to interpret images. It should be recognized that, at times, the intense subdiaphragmatic activity may interfere with detection of inferior wall

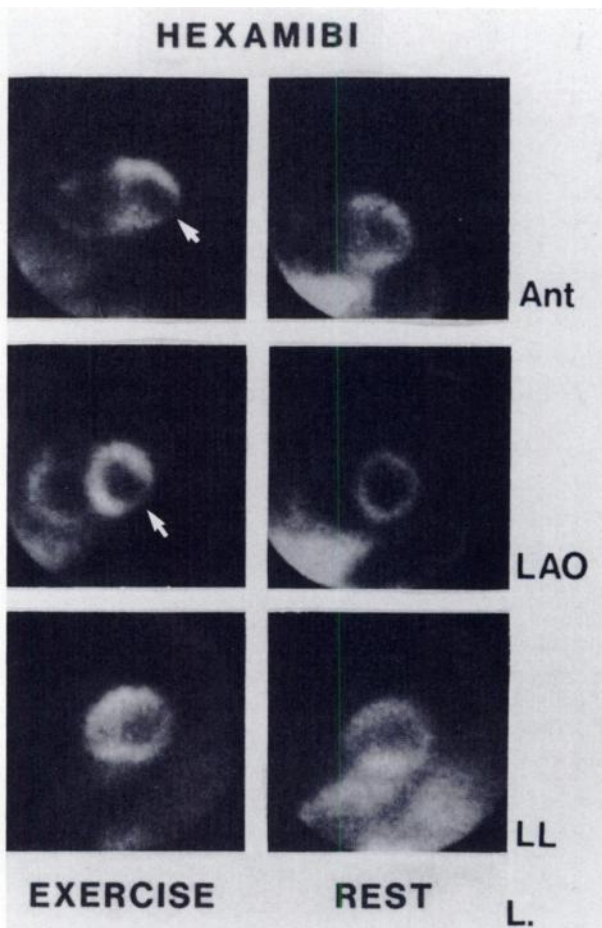
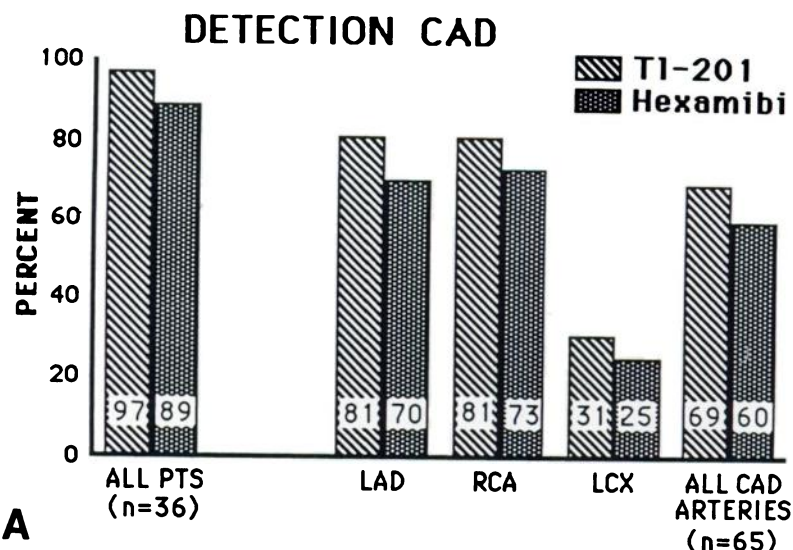
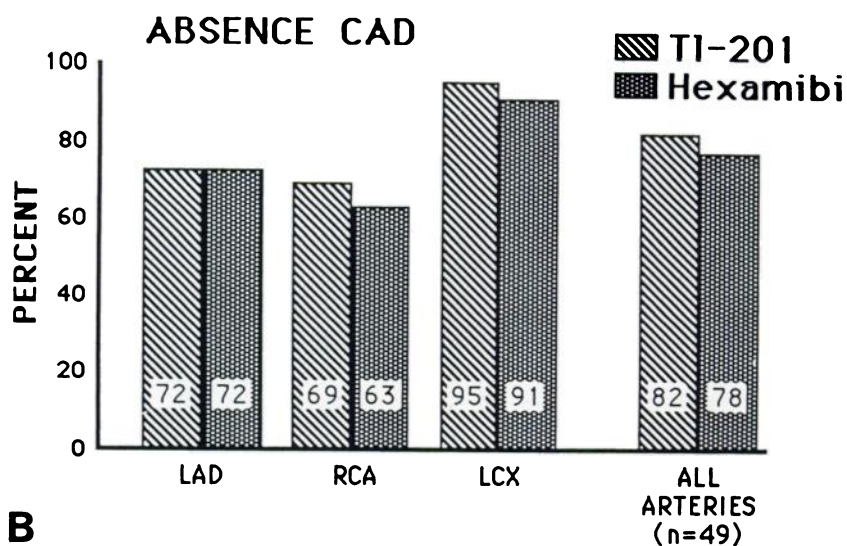


**FIGURE 4**  
[<sup>99m</sup>Tc]HEXAMIBI images after injection during exercise and at rest in Patient L with significant coronary artery disease. The myocardial perfusion images demonstrate reversible defects (arrows) involving the inferolateral and inferoapical segments.



**A**



**B**

**FIGURE 5**

**A:** Comparative *detection* rate of significant coronary artery disease by  $^{201}\text{Tl}$  and [ $^{99\text{m}}\text{Tc}$ ]HEXAMIBI (Hexamibi) stress/rest imaging. No statistically significant difference exists for either the overall detection of disease or the detection of disease in specific vascular territories (see text). **B:** Comparative identification of the *absence* of coronary artery disease for  $^{201}\text{Tl}$  and [ $^{99\text{m}}\text{Tc}$ ]HEXAMIBI (Hexamibi) stress/rest imaging. No statistically significant difference exists between the two imaging agents (see text). Abbreviations: LAD = left anterior descending coronary artery; RCA = right coronary artery; LCx = left circumflex coronary artery.

defects, in particular in images obtained within 1 hr after injection of radiopharmaceutical. In our experience, eating or drinking of milk during the hour after injection may improve the images substantially.

None of the volunteers or patients experienced sub-

jective or objective adverse reactions from the administration of the radiopharmaceutical.

Favorable patient dosimetry makes it feasible to administer a ten times higher dose (not exceeding 30 mCi) of [ $^{99\text{m}}\text{Tc}$ ]HEXAMIBI than  $^{201}\text{Tl}$ , assuring high quality

**FIGURE 6**

Comparative interpretation of three-view patient studies (38 patients, 570 segments) with  $^{201}\text{Tl}$  and [ $^{99\text{m}}\text{Tc}$ ]HEXAMIBI. Abbreviations: N = normal; I = ischemic (reversible defect); S = scar (fixed defect). A patient study was graded as I when at least one segment was graded as ischemic, and graded as S when all abnormal segments were graded as scar.

		$^{99\text{m}}\text{Tc}$ -HEXAMIBI					
		N	I	S	N	I	S
$^{201}\text{Tl}$	N	2	1	0	389	16	5
	I	3	25	4	50	41	11
	S	1	0	2	14	11	33
		Concordance 29/38 patients(76%)			463/570 segments(81%)		

(high count density, high resolution) cardiac images at rest and after exercise.

Since [ $^{99m}\text{Tc}$ ]HEXAMIBI is predominantly bound to the cytosol fraction of the myocardial cells (6), the distribution of the radiopharmaceutical remained relatively fixed in the myocardium. Several investigators have demonstrated in experimental studies that significant redistribution did not occur (4,5,15-17). Consequently, the timing of imaging after administration of [ $^{99m}\text{Tc}$ ]HEXAMIBI is not as critical as after injection of  $^{201}\text{Tl}$  for detection of myocardial perfusion defects. Moreover, the quality of the images improved over time by clearance of liver activity in the gallbladder. For practical and logistic reasons, we chose in the Phase II studies to acquire images 1 hr after injection. A disadvantage of the lack of redistribution is that for evaluation of defect reversibility (or exercise-induced ischemia) a separate and second injection of [ $^{99m}\text{Tc}$ ]HEXAMIBI is required.

The purpose of the Phase II patient study was to evaluate the feasibility of rest-exercise [ $^{99m}\text{Tc}$ ]HEXAMIBI imaging in comparison to  $^{201}\text{Tl}$  imaging in patients with angiographically proven coronary artery disease. The initial results demonstrate that 89% of 36 patients with coronary artery disease had abnormal [ $^{99m}\text{Tc}$ ]HEXAMIBI studies, compared to 97% of patients with  $^{201}\text{Tl}$ . In this limited number of patients studied by coronary angiography, the detection rate of [ $^{99m}\text{Tc}$ ]HEXAMIBI stress imaging was statistically not significantly lower than that of  $^{201}\text{Tl}$  stress imaging. Moreover, no significant differences existed in detection of disease in the vascular beds of specific coronary arteries.

On a segment-to-segment basis, complete agreement between the two imaging agents occurred in 81%. However, more myocardial segments were abnormal on  $^{201}\text{Tl}$  images than on [ $^{99m}\text{Tc}$ ]HEXAMIBI images. In addition, ischemia was more frequently, although not statistically significant, noted on  $^{201}\text{Tl}$  images than on [ $^{99m}\text{Tc}$ ]HEXAMIBI images. These trends should be further evaluated in future comparative studies.

Considering these preliminary clinical results, it should be appreciated that, by study design, a bias existed in favor of  $^{201}\text{Tl}$  imaging. The majority of patients were asked to participate in the study because they had abnormal  $^{201}\text{Tl}$  stress images. Consequently, the results of [ $^{99m}\text{Tc}$ ]HEXAMIBI stress imaging could not be better than  $^{201}\text{Tl}$  stress imaging. Furthermore, the image interpreters have had a vast experience with  $^{201}\text{Tl}$  image reading, and thus familiarity with normal variations in regional  $^{201}\text{Tl}$  distribution patterns. In contrast, the experience with [ $^{99m}\text{Tc}$ ]HEXAMIBI was limited to the patients included in this study. Moreover, the present comparison was based upon *qualitative* visual analysis only. Our initial attempts to employ the same *quantitative* methodology for [ $^{99m}\text{Tc}$ ]HEXAMIBI

images as for  $^{201}\text{Tl}$  images showed that the relatively high subdiaphragmatic activity, typical for the [ $^{99m}\text{Tc}$ ]HEXAMIBI images, caused oversubtraction and artifacts (18). Preliminary results using a modification of the interpolative background subtraction algorithm for [ $^{99m}\text{Tc}$ ]HEXAMIBI indicated that the agreement between the two imaging agents was significantly better by computer processing than by visual analysis (19).

Although in the present study every attempt was made to reproduce the exercise efforts during both tests, this was not achieved in all patients and potentially may have affected the results.

Although the present preliminary results in a limited number of patients are encouraging, it would be premature to decide whether [ $^{99m}\text{Tc}$ ]HEXAMIBI could replace  $^{201}\text{Tl}$  for clinical imaging. There has been extensive clinical experience utilizing  $^{201}\text{Tl}$  as a myocardial perfusion agent. In particular, its clinical usefulness, in conjunction with exercise testing is well established (9,20-21). Not only is  $^{201}\text{Tl}$  stress imaging successfully employed for the detection of coronary artery disease, the method provides important prognostic information with regard to the functional significance of disease (22-28). Nevertheless, [ $^{99m}\text{Tc}$ ]HEXAMIBI has certain attractive characteristics to justify further clinical evaluation in comparison with  $^{201}\text{Tl}$ . The 140-keV photon energy is optimal for gamma camera imaging and is more likely to produce high quality images. The half-life of  $^{99m}\text{Tc}$  and dosimetry of [ $^{99m}\text{Tc}$ ]HEXAMIBI make it possible to administer 10-15 times higher dose of radiopharmaceutical than with  $^{201}\text{Tl}$ . Not only does this result in better images within shorter time, but it allows combination of myocardial perfusion imaging with assessment of right and left ventricular ejection fraction by first-pass radionuclide angiocardigraphy (29). In addition, the high photon flux allows ECG-synchronized image acquisition and analysis of regional wall motion from cine display of the perfusion images (as is routinely done with equilibrium blood-pool studies) (30-35). Furthermore, since [ $^{99m}\text{Tc}$ ]HEXAMIBI remains relatively fixed in the myocardium without redistribution, providing information on regional myocardial blood flow at the time of administration, this radiopharmaceutical has the potential to be superior to  $^{201}\text{Tl}$  for assessment of myocardium at risk in the setting of acute interventions such as thrombolytic therapy for acute myocardial infarction (26) or coronary angioplasty. For instance, the radiopharmaceutical could be administered during the intervention, while imaging could be postponed and be performed at a later, more convenient time, without loss of information on distribution of myocardial blood flow at the time it was injected.

The high photon flux and energy of [ $^{99m}\text{Tc}$ ]HEXAMIBI are ideally suited for single photon emission tomography. Preliminary results indicate excellent im-

age quality and closer agreement with  $^{201}\text{Tl}$  tomography in detection of coronary artery disease than by planar imaging (32,37–39). Nevertheless, for practical application, it is relevant to further delineate the clinical efficacy of planar imaging with [ $^{99\text{m}}\text{Tc}$ ]HEXAMIBI. A multicenter Phase III trial involving both planar and tomographic imaging is presently ongoing to further define the usefulness of myocardial imaging with [ $^{99\text{m}}\text{Tc}$ ]HEXAMIBI in patients with coronary artery disease.

## APPENDIX

### Participating Centers in [ $^{99\text{m}}\text{Tc}$ ]HEXAMIBI Phase I and II Studies

Yale University School of Medicine, New Haven, Connecticut, Investigators: Frans J. Th. Wackers, MD and Barry L. Zaret, MD, David S. Kayden, MD. Cedars-Sinai Medical Center, Los Angeles, California, Investigators: Daniel S. Berman, MD, Jamshid Maddahi, MD. University of Virginia Medical Center, Charlottesville, Virginia, Investigators: George A. Beller, MD, C. David Teates, MD, Denny D. Watson, PhD. Massachusetts General Hospital, Boston, Massachusetts, Investigators: Charles Boucher, MD, H. William Strauss, MD. Brigham & Women's Hospital, Boston, Massachusetts, Investigators: B. Leonard Holman, MD, Michel Picard, MD. Centre Hospitalier Universitaire Vaudois, Lausanne, Switzerland, Investigators: Angelika Bischof-Delaloye, MD, Bernard Delaloye, MD. University of Basel, Basel, Switzerland, Investigators: R. Fridrich, MD, J. Muller-Brand, MD, M. Pfisterer, MD. Ospedale Niguarda, Milano, Italy, Investigator: Eugenio Inglese, MD. The Groby Road Hospital, Leicester, England, Investigator: M. Khalil, MD. Guy's Hospital, London, England, Investigator: M.N. Maisey, MD. University of Amsterdam, Amsterdam, The Netherlands, Investigators: S.C.C. Reinders Folmer, MD, J.B. van der Schoot, MD.

## ACKNOWLEDGMENTS

The secretarial assistance of Mrs. Wendy Rosenberg is greatly appreciated. [ $^{99\text{m}}\text{Tc}$ ]HEXAMIBI (Cardiolite) was manufactured and supplied by Du Pont Company, Diagnostic Imaging, No. Billerica, Massachusetts.

Human dosimetry was calculated by Michael Stabin of the Radiopharmaceutical Internal Dose Information Center, Oak Ridge Associated Universities, Oak Ridge, TN.

## REFERENCES

- Holman BL, Jones AG, Lister-James J, et al. A new Tc-99m-labeled myocardial imaging agent, hexakis (t-Butylisonitrile)-technetium(I) [Tc-99m TBI]: initial experience in the human. *J Nucl Med* 1984, 25:1350–1355.
- Holman BL, Sporn V, Jones AG, et al. Myocardial imaging with technetium-99m CPI: initial experience in the human. *J Nucl Med* 1987; 28:13–18.
- Deutsch E, Vanderheyden JL, Gerundini P, et al. Development of nonreducible technetium-99m(III) cations as myocardial perfusion imaging agents: initial experience in humans. *J Nucl Med* 1987; 28:1870–1880.
- Mousa SA, Cooney JM, Williams SJ. Flow-distribution characteristics of Tc-99m-hexakis-2-methoxy, 2-methylpropyl isonitrile in animal models of myocardial ischemia and reperfusion. *J Am Coll Cardiol* 1987; 9:137A.
- Mousa SA, Cooney JM, Williams SJ. Regional myocardial distribution of RP-30 in animal models of myocardial ischemia and reperfusion [Abstract]. *J Nucl Med* 1987; 28:620.
- Mousa SA, Maina M, Brown BA, et al. Retention of RP-30 in the heart may be due to binding to a cytosolic protein [Abstract]. *J Nucl Med* 1987; 28:619.
- Piwnica-Worms D, Kronauge JF, Holman BL, et al. Hexakis (Carbomethoxyisopropylisonitrile) technetium(I), a new myocardial perfusion imaging agent: binding characteristics in cultured chick heart cells. *J Nucl Med* 1988; 29:55–61.
- Maublant JC, Gachon P, Moins N. Hexakis (2-methoxy isobutylisonitrile) technetium-99m and thallium-201 chloride: uptake and release in cultured myocardial cells. *J Nucl Med* 1988; 29:48–54.
- Wackers FJTh, Fetterman RC, Mattera JA, et al. Quantitative planar thallium-201 stress scintigraphy: a critical evaluation of the method. *Semin Nucl Med* 1985; 15:46–66.
- Loevinger R and Berman M. A revised schema for calculating the absorbed dose from biologically distributed radionuclides. MIRD Pamphlet No. 1, Revised. New York: Society of Nuclear Medicine, 1976.
- Cloutier RJ, Watson EE, Rohrer RH, et al. Calculating the radiation dose to an organ. *J Nucl Med* 1973; 14:53–55.
- Dunn RF, Freedman B, Bailey IK, Uren RF, Kelly DT. Exercise thallium imaging: location of perfusion abnormalities in single-vessel coronary disease. *J Nucl Med* 1980; 21:717–722.
- Maddahi J, Garcia EV, Berman DS, Waxman A, Swan HJC, Forrester J. Improved noninvasive assessment of coronary artery disease by quantitative analysis of regional stress myocardial distribution and washout of thallium-201. *Circulation* 1981; 64:924–935.
- Atkins HL, Budinger TF, Lebowitz E, et al. Thallium-201 for medical use. Part 3: human distribution and physical imaging properties. *J Nucl Med* 1977; 18:133–140.
- Okada RD, Glover D, Gaffney T, et al. Myocardial kinetics of technetium-99m-hexakis-2-methoxy-2-methylpropyl-isonitrile. *Circulation* 1988; 77:491–498.
- Marshall RC, Leidholdt Jr EM, Barnett CA. Single pass myocardial extraction and retention of a Tc-99m isonitrile vs. Tl-201. *Circulation* 1987; 76:IV–218.
- Quan-Sheng L, Frank TL, Franceschi D, et al. Technetium-99m methoxyisobutyl isonitrile (RP30) for quantification of myocardial ischemia and reperfusion in dogs. *J Nucl Med* 1988; 29:1539–1548.
- Koster K, Wackers FJTh, Fetterman R, Watson DD, Smith WH, Mattera J. Interpolative background subtraction as used for Tl-201 imaging creates major inaccuracy in quantitative Tc-99m isonitrile imaging. *J Am Coll Cardiol* 1988; 11:33A.
- Koster K, Wackers FJTh, Mattera J, et al. Quantitative analysis of planar Tc-99m-isonitrile images. Necessity of new normal database and modified background correction [Abstract]. *J Nucl Med* 1988; 29:804.

20. Maddahi J, Abdulla A, Garcia EV, Swan HJC, Berman DS. Noninvasive identification of left main and triple vessel coronary artery disease: improved accuracy using quantitative analysis of regional myocardial stress distribution and washout of thallium-201. *J Am Coll Cardiol* 1986; 7:53-60.
21. Van Train KF, Berman DS, Garcia EV, et al. Quantitative analysis of stress thallium-201 myocardial scintigrams: a multicenter trial. *J Nucl Med* 1986; 27:17-25.
22. Brown KA, Boucher CA, Okada RD, et al. Prognostic value of exercise thallium-201 imaging in patients presenting for evaluation of chest pain. *J Am Coll Cardiol* 1983; 1:994-1001.
23. Gibson RS, Watson DD, Craddock GB, et al. Prediction of cardiac events after uncomplicated myocardial infarction: a prospective study comparing predischARGE exercise thallium-201 scintigraphy and coronary angiography. *Circulation* 1983; 68:321-326.
24. Ladenheim ML, Pollock BH, Rozanski A, et al. Extent and severity of myocardial hypoperfusion as predictors of prognosis in patients with suspected coronary artery disease. *J Am Coll Cardiol* 1986; 7:464-471.
25. Staniloff HM, Forrester JS, Berman DS, et al. Prediction of death, myocardial infarction, and worsening chest pain using thallium scintigraphy and exercise electrocardiography. *J Nucl Med* 1986; 27:1842-1848.
26. Wackers FJTh, Russo DJ, Russo D, et al. Prognostic significance of normal quantitative planar thallium-201 stress scintigraphy in patients with chest pain. *J Am Coll Cardiol* 1985; 6:27-30.
27. Pamela FX, Gibson RS, Watson DD, et al. Prognosis with chest pain and normal thallium-201 exercise scintigrams. *Am J Cardiol* 1985; 55:920-926.
28. Gill JB, Ruddy TD, Newell JB, et al. Prognostic importance of thallium uptake by the lungs during exercise in coronary artery disease. *N Engl J Med* 1987; 317:1485-1489.
29. Balino NP, Sporn V, Kuschnir E, et al. Simultaneous test of ventricular function and myocardial perfusion with Tc-99m-RP-30 [Abstract]. *J Nucl Med* 1987; 28:662.
30. Wackers FJ, Mattera JA, Bowman L, Zaret BL. Gated Tc-99m-isonitrile myocardial perfusion imaging: disparity between endo-, and epicardial wall motion. *Circulation* 1987; 76:IV-203.
31. Merz R, Maddahi J, Roy L, Berman DS. Gated RP-30 perfusion study after stress predicts myocardial viability. *J Am Coll Cardiol* 1987; 9:27A.
32. Corbett JR, Henderson EB, Akers MS, et al. Gated tomography with technetium-99m RP-30A in patients with myocardial infarcts: assessment of myocardial perfusion and function. *Circulation* 1987; 76:IV-217.
33. Camargo EE, Hironaka FH, Giorgi MCP, et al. Amplitude analysis of stress <sup>99m</sup>Tc-MIBI (RP-30A) in the assessment of coronary artery disease (CAD) [Abstract]. *J Nucl Med* 1988; 29:805.
34. Roseman H, Chesler D, LaRaia P, et al. Determination of left ventricular function with technetium-99m isonitrile dynamic imaging [Abstract]. *J Nucl Med* 1988; 29:805.
35. Henze E, Clausen M, Weller R, et al. Quantification of LV function from gated planar Tc-99m RP-30 studies by means of the contraction fraction [Abstract]. *J Nucl Med* 1988; 29:818.
36. Kayden DS, Mattera JA, Zaret BL, Wackers FJTh. Demonstration of reperfusion after thrombolysis with Tc-99m isonitrile myocardial imaging. *J Nucl Med* 1988; 29:1865-1867.
37. Kiat H, Maddahi J, Roy LT et al. Comparison of technetium-99m methoxy isobutyl isonitrile and thallium-201 for evaluation of coronary artery disease by planar and tomographic methods. *Am Heart J* 1989; 117:1-11.
38. Stirner H, Buell U, Kleinhans E, et al. Myocardial kinetics of <sup>99m</sup>Tc-hexakis-(2-methoxy-isobutyl-isonitrile) (HMIBI) in patients with coronary heart disease: a comparative study versus <sup>201</sup>Tl with SPECT. *Nucl Med Commun* 1988; 9:15-23.
39. Karcher G, Bertrand A, Moretti JL, et al. Comparative study by two independent observers of the uptake abnormalities of <sup>201</sup>Tl and Tc-99m-MIBI in 81 patients with coronary artery disease [Abstract]. *J Nucl Med* 1988; 29:793.